Referring Expression Comprehension via Cross-Level Multi-Modal Fusion

Peihan Miao
Zhejiang University, China
peihan.miao@zju.edu.cn

Wei Su
Zhejiang University, China
weisuzju@zju.edu.cn

Lian Wang
Zhejiang University, China
wanglian1999@zju.edu.cn

Yongjian Fu*
Zhejiang University, China
yjfu@zju.edu.cn

Xi Li*
Zhejiang University, China
xilizju@zju.edu.cn

ABSTRACT

As an important and challenging problem in vision-language tasks, referring expression comprehension (REC) aims to localize the target object specified by a given referring expression. Recently, most of the state-of-the-art REC methods mainly focus on multi-modal fusion while overlooking the inherent hierarchical information contained in visual and language encoders. Considering that REC requires visual and textual hierarchical information for accurate target localization, and encoders inherently extract features in a hierarchical fashion, we propose to effectively utilize the rich hierarchical information contained in different layers of visual and language encoders. To this end, we design a Cross-level Multi-modal Fusion (CMF) framework, which gradually integrates visual and textual features of multi-layer through intra- and inter-modal. Experimental results on RefCOCO, RefCOCO+, RefCOCOg, and ReferItGame datasets demonstrate the proposed framework achieves significant performance improvements over state-of-the-art methods.

CCS CONCEPTS

• **Computing methodologies → Matching**.

KEYWORDS

vision-language task, referring expression comprehension, hierarchical information, cross-level multi-modal fusion

1 INTRODUCTION

Referring expression comprehension (REC) [8, 35, 50, 51, 54] is a challenging task that aims at localizing the target object specified by a given referring expression, which can underpin a diverse set of vision-language tasks such as visual question answering [1, 13, 61], image captioning [39, 53], and image retrieval [46]. In addition, the development of REC will contribute to the advances in fields such as robotics, human-computer interaction, and early education in the physical world.

As a language-to-visual precise matching problem, REC generally requires hierarchical information of both visual and textual modal to realize target localization. For instance, as shown in Fig. 1, the visual branch needs to provide visual hierarchical information including color and texture (*e.g.* people's clothing) at the low level, and semantic or relationships of instances (*e.g.* people's gender and relative positions) at the high level. The language branch also needs to take into account textual hierarchical information to capture both the simple phrase-level information (*e.g.* "lady" and "white shirts") and relatively complex long-range information derived from the whole sentence (*e.g.* the "lady" is "next to man in hat"). Overlooking hierarchical information in images or referring expressions may lead to suboptimal results, as shown in our experiments.

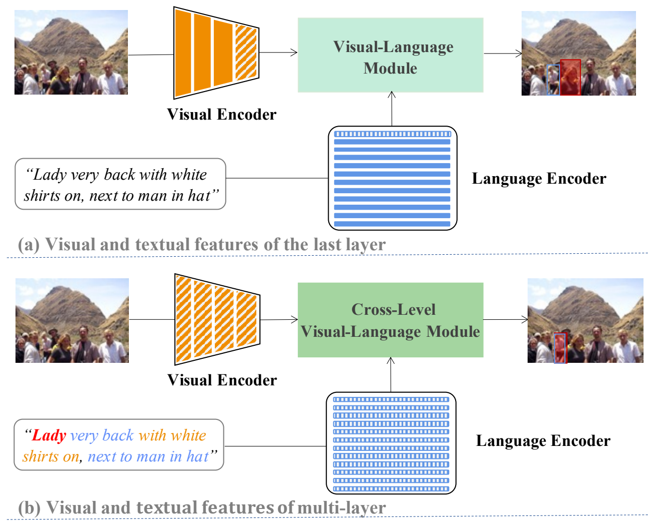

Figure 1: State-of-the-art methods typically extract features from the last layer of visual and language encoders (a). Our method exploits the rich hierarchical information contained in visual and language encoders (b).

On the other hand, when reviewing the general REC framework [8] (including visual encoder, language encoder, multi-modal fusion module and prediction head), it can be observed that the visual and language encoders inherently extract features in a hierarchical fashion. A long line of works indicates that visual encoders like ResNet [16] tend to capture semantic information in deeper layers, and detailed information in shallower layers [14, 30, 56]. Meanwhile, transformer-based [48] language encoders like BERT [9] can capture surface (phrase-level) information in lower layers, syntactic information in middle layers, and semantic information in higher layers [21]. We claim that these inherent property of visual and language encoders are potential to tackle the above requirement of REC task, which is the main topic of this paper.

Recent state-of-the-art methods [8, 11, 22, 25, 47, 51] mainly focus on designing multi-modal fusion modules to better fuse the

* Corresponding author.

visual and textual features, and thereby realize language-to-visual localization, as shown in Fig. 1 (a). Despite achieving high performance, such methods typically extract features from one specific layer (usually the last layer) of visual and language encoders, which make it difficult to capture rich hierarchical information as REC needs. To remedy it, in this paper, we propose to effectively utilize the rich hierarchical information contained in different layers of visual and language encoders, and design an effective cross-level multi-modal fusion framework to improve REC performance, as shown in Fig. 1 (b).

When faced with visual and textual features of multi-layer, how to effectively realize multi-modal fusion has become a challenge. If the features are simply fused, a lot of hierarchical information will be lost. To this end, we design a Cross-level Multi-modal Fusion (CMF) framework, which gradually integrates visual and textual features at different layers through intra- and inter-modal to improve REC performance. Specifically, considering that visual features of different layers may require diverse hierarchical textual features for multi-modal interaction, and the number of textual and visual features belongs to many-to-few, we design a language-adaptive fusion module (LAFM) to perform intra-modal fusion of textual features, and assign adaptively fused textual features to visual features of each layer. After obtaining visual features and their corresponding textual features, we design two successive processes, *i.e.* grouping multi-modal interaction and cross-level multi-modal fusion, to perform intra- and inter-modal fusion. In the grouping multi-modal interaction, we propose a transformer-based visual-language interaction module (VLIM) to realize the interaction of visual and textual features. Then, we fuse all visual and textual features updated by VLIM into the final visual and textual features, respectively. The final visual and textual features are concatenated and input into the transformer-based visual-language fusion module (VLFM) to achieve cross-level multi-modal fusion. Extensive experiments demonstrate the effectiveness of our method, which outperforms state-of-the-art methods by a large margin on the popular RefCOCO [55], RefCOCO+ [55], RefCOCOg [36], and ReferItGame [23] datasets.

Conclusively, our contributions are three-fold:

- We propose to effectively utilize the inherent hierarchical information contained in visual and language encoders for accurate language-to-visual localization.
- We design a Cross-level Multi-modal Fusion (CMF) framework, which gradually integrates multi-layer visual and textual features containing rich hierarchical information.
- Extensive experiments demonstrate the effectiveness of our method, which significantly outperforms state-of-the-art methods on the four popular datasets.

2 RELATED WORK

2.1 Referring Expression Comprehension

Recent advancements in REC can be divided into two research directions: two-stage methods [3, 17, 18, 29, 54] and one-stage methods [8, 25, 27, 35, 51, 52]. We briefly introduce the contents of the two research directions separately in the following.

Two-stage methods. Most conventional REC methods include two stages [3, 17, 29, 54], *i.e.*, the generation of candidate boxes and the selection of the best matching boxes. In the first stage, numerous candidate boxes are generated by pre-training object detector framework, *e.g.* Faster-RCNN [43] or Mask-RCNN [15]. In the second stage, the candidate box that best matches the given referring expression will be regarded as the target box. MAttNet [54] proposes the Modular Attention Network that uses language-based and vision-based attention to model the appearance, location, and relationship of the objects. Ref-NMS [3] generates expression-aware proposals at the first stage to improve the performance of REC, which can be integrated into state-of-the-art two-stage methods as a plug-and-play module. Despite achieving excellent performance, the two-stage methods are restricted by the accuracy of the candidate boxes and the matching correctness of the candidate boxes and the referring expression.

One-stage methods. Recently, one-stage methods [8, 25, 27, 35, 51, 52] that directly predict the target box have been used to alleviate the limitations of the aforementioned two-stage methods. TransVG [8] proposes a transformer-based [48] framework that contains visual, linguistic, and visual-linguistic transformers to directly regress the coordinates of the target box. ReSC [51] proposes to reduce referring ambiguity by exploiting multiple rounds of query with visual and textual features in the face of complex referring expressions. Referring Transformer [25] propose the one-stage multi-task frameworks, which use REC and referring expression segmentation (RES) to jointly learn. Despite achieving good performance, such methods mainly focus on multi-modal fusion and overlook the inherent hierarchical information contained in visual and language encoders.

2.2 Transformer

Transformer [48], first introduced for neural machine translation, has sparked a huge research boom in recent years. Transformer-based methods have achieved state-of-the-art performance in natural language tasks [6, 7, 9, 59]. Inspired by the great success in natural language tasks, a large number of transformer-based vision tasks, such as image classification [10, 32, 40], object detection [2, 60] and panoptic segmentation [5, 49], have been researched. In addition, transformer-based multi-modal pre-training methods [4, 26, 34] for visual-language tasks have gradually emerged. As the core component of transformer, attention [48] is developed to capture long-range interactions in the context and both correspondence of tokens across modalities. Recently, some state-of-the-art REC methods [8, 22, 25] have shown that transformer can capture intra- and inter-modal contexts homogeneously across visual and textual modalities. Inspired by this, we utilize the transformer-based modules in our framework to achieve effective cross-level multi-modal fusion.

3 METHOD

In this section, we illustrate the proposed Cross-level Multi-modal Fusion (CMF) framework in detail. First, we briefly introduce an overview of the proposed framework in the Section 3.1. Then, we describe the proposed language-adaptive fusion in the Section 3.2.

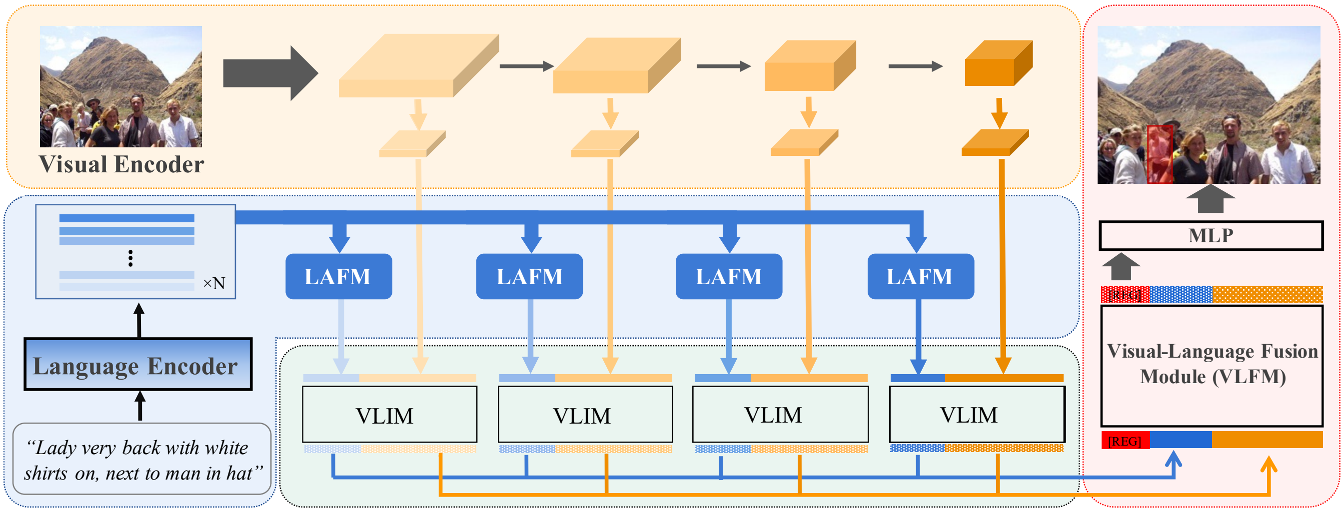

Figure 2: Illustration of our proposed Cross-level Multi-modal Fusion (CMF) framework. The whole framework consists of visual encoder, language encoder, language-adaptive fusion module (LAFM), visual-language interaction module (VLIM), visual-language fusion module (VLFM) and prediction head. Concretely, the visual and language encoders extract visual and textual features of different layers, respectively. Each LAFM is used to assign adaptively fused textual features to the corresponding visual features, and VLIM is used for multi-modal interaction. VLFM uses the final visual and textual features to achieve cross-level multi-modal fusion. A prediction head composed of a multi-layer perceptron converts the [REG] token output by VILM into the coordinates of the target box. Best viewed in color.

Next, we elaborate on the specific processes for the cross-level multi-modal fusion in the Section 3.3. Finally, we detail the optimization of the whole framework in the Section 3.4.

3.1 Overview

Given an image and a referring expression, the goal of our framework is to directly regress the coordinates of the target box, where the whole framework consists of six main components: visual encoder, language encoder, language-adaptive fusion module (LAFM), visual-language interaction module (VLIM), visual-language fusion module (VLFM) and prediction head, as illustrated in Fig. 2.

Specifically, visual encoder based on ResNet [16] extracts the visual features from the last four stages. To facilitate subsequent operations, we use 3×3 convolution, batch normalization [20], ReLU and bilinear downsampling to obtain visual features $\{F_v^i\}_{i=1}^4$ of same dimension $\mathbb{R}^{C\times H\times W}$, where C, H and W represent the channels, height and width, respectively. Language encoder based on N-layer BERT [9] extracts the textual features $\{F_l^j\}_{j=1}^N$ of the same dimension $\mathbb{R}^{Q\times L}$, where Q and L represent the channels and length, respectively. LAFM adaptively fuses textual features from N-layer textual features for each visual features F_v^i to obtain $\{(F_v^i, \dot{F}_l^i)\}_{i=1}^4$. Each $(F_v^i, \dot{F}_l^i)$ uses its VLIM for multi-modal interaction, resulting in $\{(\bar{F}_v^i, \bar{F}_l^i)\}_{i=1}^4$. All visual and textual features are fused into the visual features $\widetilde{F}_v$ and textual features $\widetilde{F}_l$, respectively. The learnable embedding [REG] token, visual features $\widetilde{F}_v$ and textual features $\widetilde{F}_l$ are concatenated and input into the VLFM to achieve cross-level multi-modal fusion. In the end, the prediction head composed of a three-layer perceptron converts the [REG] token output by VLFM into the coordinates of the target box $\hat{\boldsymbol{b}} = (\hat{x}, \hat{y}, \hat{h}, \hat{w})$.

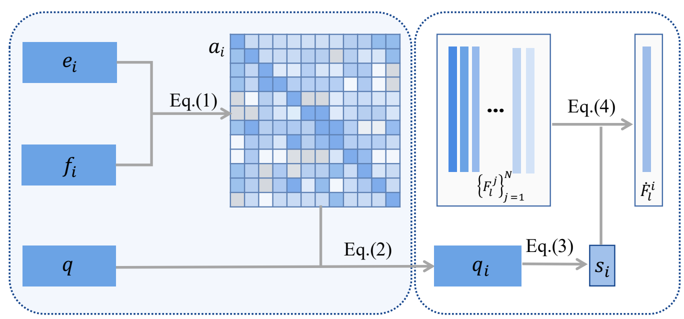

Figure 3: Illustration of textual feature fusion in our proposed language-adaptive fusion module (LAFM).

3.2 Language-Adaptive Fusion

The visual and textual features extracted from the visual and language encoders at different layers contain hierarchical information [14, 21, 30, 56]. Considering that visual features of different layers may require diverse hierarchical textual features for multi-modal interaction, and the number of textual and visual features belongs to many-to-few, we use language-adaptive fusion module (LAFM) to perform intra-modal fusion of textual features, and assign the adaptively fused textual features to the corresponding visual features.

Concretely, for visual features F_v^i, i-th LAFM is used to adaptively fuse the textual features $\{F_l^j\}_{j=1}^N$, and obtain the adaptively fused textual features $\dot{F}_l^i \in \mathbb{R}^{Q\times L}$. We extract the [CLS] token from textual features of each layer, and stack them to obtain $q \in \mathbb{R}^{N\times Q}$, where [CLS] token contains the understanding of the entire referring expression. To achieve better textual feature fusion, we design the structure as shown in Fig. 3. We first use the linear projection layer and L2 normalization on q to obtain $e_i \in \mathbb{R}^{N\times Q}$ and $f_i \in \mathbb{R}^{N\times Q}$, respectively. Then, we utilize language-level self-attention to establish the affinity matrix $a_i \in \mathbb{R}^{N\times N}$ between textual features at different layers. We have

$$a_i = \mathrm{softmax}(e_i f_i^T), \tag{1}$$

where $f_i^T \in \mathbb{R}^{Q\times N}$ represents the transpose of f_i, and a_i contains the correlation coefficients between textual features of each layer. Next, we use affinity matrix a_i and q to obtain the $q_i \in \mathbb{R}^{N\times Q}$ through Eq. (2):

$$q_i = a_i q. \tag{2}$$

After obtaining q_i, we use Eq. (3) to obtain an N-dimensional vector s_i, each value of which corresponds to the fusion weight of textual features of each layer.

$$s_i = \mathrm{softmax}(\mathrm{ReLU}(\mathrm{BN}(q_i w_i^1 + b_i^1)) w_i^2 + b_i^2), \tag{3}$$

where w_i^1, b_i^1, w_i^2 and b_i^2 are the learnable parameters in the two linear projection layers. In addition, BN and ReLU represent batch normalization [20] and ReLU operations, respectively. Last, we use s_i and hierarchical textual features $\{F_l^j\}_{j=1}^N$ to obtain fused textual features through Eq. (4),

$$\dot{F}_l^i = \sum_{j=1}^{N} s_i^j F_l^j, \tag{4}$$

where $\dot{F}_l^i$ is used as the adaptively fused textual features corresponding to visual features F_v^i. After language-adaptive fusion, we can obtain $\{(F_v^i, \dot{F}_l^i)\}_{i=1}^4$ to achieve the following cross-level multi-modal fusion, as depicted in Section 3.3.

3.3 Cross-Level Multi-Modal Fusion

After obtaining visual features of each layer and their corresponding textual features, we need to effectively perform multi-modal fusion to improve REC performance. To this end, we propose two successive processes, *i.e.* grouping multi-modal interaction and cross-level multi-modal fusion, to achieve intra- and inter-modal fusion, as shown in Fig. 2.

Specifically, in the grouping multi-modal interaction, we propose the visual-language interaction module (VLIM) including a stack of two transformer encoder layers. Each $(F_v^i, \dot{F}_l^i)$ is first converted into visual tokens and textual tokens separately. Then we use two linear projection layers to project visual and textual tokens into $\boldsymbol{v}_i \in \mathbb{R}^{C_0\times HW}$ and $\boldsymbol{t}_i \in \mathbb{R}^{C_0\times L}$ with same channel dimension C_0, respectively. We formulate the joint input tokens of the i-th VLIM as:

$$z_i = [\,\underbrace{t_i^1, t_i^2, \dots, t_i^L}_{\text{textual tokens } \boldsymbol{t}_i}, \overbrace{v_i^1, v_i^2, \dots, v_i^{HW}}^{\text{visual tokens } \boldsymbol{v}_i}], \tag{5}$$

where we add sinusoidal position encodings for visual tokens to maintain the position information of visual features. z_i is used as the input of VLIM to perform the intra- and inter-modality interaction. We recover the visual and textual features of the VLIM output and obtain $\{(\bar{F}_v^i, \bar{F}_l^i)\}_{i=1}^4$.

In the cross-level multi-modal fusion, we propose the visual-language fusion module (VLFM) including a stack of six transformer encoder layers. All visual and textual features are concatenated and projected into the final visual features $\widetilde{F}_v \in \mathbb{R}^{C_0\times H\times W}$ and textual features $\widetilde{F}_l \in \mathbb{R}^{C_0\times L}$, respectively. We convert $\widetilde{F}_v$, $\widetilde{F}_l$ into visual tokens $\dot{\boldsymbol{v}} \in \mathbb{R}^{C_0\times HW}$ and textual tokens $\dot{\boldsymbol{t}} \in \mathbb{R}^{C_0\times L}$, respectively. We formulate the joint input tokens of the VLFM as:

$$z' = [r,\, \underbrace{\dot{t}^1, \dot{t}^2, \dots, \dot{t}^L}_{\text{textual tokens } \dot{\boldsymbol{t}}}, \overbrace{\dot{v}^1, \dot{v}^2, \dots, \dot{v}^{HW}}^{\text{visual tokens } \dot{\boldsymbol{v}}}], \tag{6}$$

where r represents a learnable embedding [REG] token, and we also add sinusoidal position encodings for visual tokens to maintain the position information of visual features. z' is used as the input of VLFM to perform the intra- and inter-modality fusion. [REG] token containing the hierarchical information of visual and textual features are used to achieve language-to-visual localization.

3.4 Optimization

The [REG] token output by the VLFM directly predicts the target box $\hat{\boldsymbol{b}} = (\hat{x}, \hat{y}, \hat{h}, \hat{w})$ through a three-layer perceptron, and ground-truth box $\boldsymbol{b} = (x, y, h, w)$ is used to supervise the training of the framework. The whole framework is optimized end-to-end by using L1 loss and Generalized IoU loss [44]:

$$\mathcal{L} = \lambda_{L1}\mathcal{L}_{L1}(\boldsymbol{b}, \hat{\boldsymbol{b}}) + \lambda_{giou}\mathcal{L}_{giou}(\boldsymbol{b}, \hat{\boldsymbol{b}}). \tag{7}$$

where λ_{L1} and λ_{giou} control the weighting of the two losses.

4 EXPERIMENTS

4.1 Datasets and Evaluation Protocol

Datasets. For the task of REC, we conduct experiments with the widely-used RefCOCO [55], RefCOCO+ [55], RefCOCOg [36], and ReferItGame [23] datasets. RefCOCO, RefCOCO+, and RefCOCOg are collected from MS-COCO [28], whereas ReferItGame is collected from SAIAPR-12 [12]. RefCOCO and RefCOCO+ obtained from the interactive game interface include the train, val, testA, and testB sets, where images containing multiple people are in the testA set and those containing objects of other categories are in the testB set. RefCOCOg collected in a non-interactive setting has two split datasets, RefCOCOg-Google [37] and RefCOCOg-umd [38]. RefCOCOg-Google contains the train and val-g sets, two of which have overlapping images. RefCOCOg-umd has no overlapping images in the train, val-u and test-u sets. RefCOCOg generated in non-interactive setting provides longer referring expressions than RefCOCO and RefCOCO+. Follow a cleaned version of split [19, 45], ReferItGame has the train, val, and test sets. We use the val set of ReferItGame for ablation analysis, and use other sets for performance comparisons with state-of-the-art methods.

Table 1: Comparison with state-of-the-art methods on RefCOCO [55], RefCOCO+ [55], RefCOCOg [36] and ReferItGame [23]. * represents ImageNet [24] pre-training, and MS-COCO [28] pre-training is used for the rest methods. Note that when the visual backbone is pretrained on MS-COCO, overlapping images of the val/test sets of the corresponding datasets are excluded. We highlight the best and second best performance in the red and blue colors.

Methods	Venue	Backbone	RefCOCO			RefCOCO+			RefCOCOg			ReferItGame
			val	testA	testB	val	testA	testB	val-g	val-u	test-u	test
Multi-task:												
MCN [35]	CVPR20	DarkNet-53	80.08	82.29	74.98	67.16	72.86	57.31	-	66.46	66.01	-
RT* [25]	NeurIPS21	ResNet-101	82.23	85.59	76.57	71.58	75.96	62.16	-	69.41	69.40	71.42
PFOS+Speaker* [47]	TMM22	ResNet-101	78.44	81.94	73.61	65.86	72.43	55.26	64.53	67.89	67.63	67.90
Two-stage:												
MAttNet [54]	CVPR18	ResNet-101	76.65	81.14	69.99	65.33	71.62	56.02	-	66.58	67.27	29.04
DDPN [57]	IJCAI18	ResNet-101	76.80	80.10	72.40	64.80	70.50	54.01	-	-	-	63.00
RvG-Tree [17]	TPAMI19	ResNet-101	75.06	78.61	69.85	63.51	67.45	56.66	-	66.95	66.51	-
CM-Att-Erase [31]	CVPR19	ResNet-101	78.35	83.14	71.32	68.09	73.65	58.03	-	67.99	68.67	-
Ref-NMS [3]	AAAI21	ResNet-101	80.70	84.00	76.04	68.25	73.68	59.42	-	70.55	70.62	-
One-stage:												
FAOA [52]	ICCV19	DarkNet-53	72.54	74.35	68.50	56.81	60.23	49.60	56.12	61.33	60.36	60.67
RCCF [27]	CVPR20	DLA-34	-	81.06	71.85	-	70.35	56.32	-	-	65.73	63.79
ReSC-Large [51]	ECCV20	DarkNet-53	77.63	80.45	72.30	63.59	68.36	56.81	63.12	67.30	67.20	64.60
HFRN [42]	ACM MM20	ResNet-101	79.76	83.12	75.51	66.80	72.53	57.09	-	69.71	69.08	-
RealGIN [58]	TNNLS21	DarkNet-53	77.25	78.70	72.10	62.78	67.17	54.21	-	62.75	62.33	-
TransVG [8]	ICCV21	ResNet-101	81.02	82.72	78.35	64.82	70.70	56.94	67.02	68.67	67.73	70.73
VGTR [11]	ICME22	ResNet-101	79.30	82.16	74.38	64.40	70.85	55.84	64.05	66.83	67.28	-
Ours	-	ResNet-50	83.76	87.31	78.68	73.05	78.15	62.79	72.21	74.75	74.01	73.13
Ours	-	ResNet-101	84.59	87.33	79.94	73.64	78.26	63.24	72.54	76.33	74.67	73.93

Table 2: Ablation study of each main component in our framework on the ReferItGame val set.

$\{F_v^i\}_{i=1}^4$	VLIM(One Layer)	LAFM	VLIM(Two Layers)	*Acc*@0.5
				72.74
✓				74.04
✓	✓			75.03
✓	✓	✓		75.73
✓		✓	✓	**76.19**

Table 3: Ablation study of the language-adaptive fusion module on the ReferItGame val set.

Design of the language-adaptive fusion module	*Acc*@0.5
Textual Features of Last Layer	75.03
N Learnable Parameters + Softmax	75.11
CLS + Softmax	75.25
CLS + Self-Attention + Softmax	**75.73**
MAX + Self-Attention + Softmax	75.22
MEAN + Self-Attention + Softmax	75.30

Evaluation Protocol. Following the previous works [8, 27, 51], we use *Acc*@0.5 to evaluate the performance of the network. Concretely, given an image and a referring expression, a predicted bounding box is regarded correct if intersection-over-union (IoU) with the ground-truth bounding box is greater than 0.5.

4.2 Implementation Details

Training. The whole network is end-to-end optimized by AdamW [33] with weight decay of 1e-4. ResNet-50 or ResNet-101 [16] pretrained on MS-COCO [28] is used as visual encoder to extract visual features from the last four stages. In particular, during pre-training of the visual encoder, images in the val/test sets overlapping with MS-COCO will be removed. The uncased base of N-layer BERT [9] is used as language encoder to extract textual features, where N is 12. Visual-language interaction module (VLIM) contains a stack of two transformer encoder layers and two linear projection layers. Visual-language fusion module (VLFM) contains a stack of six transformer encoder layers and two linear projection layers. We set an initial learning rate of 1e-5 for the visual and language encoders, and 1e-4 for the remaining components. The model is trained for 140 epochs with batch-size of 128, where the learning rate is reduced by a factor of 10 at 100 epochs. The weights of λ_{L1} and λ_{giou} are set to 1. The channel dimension C_0 is set to 256. The input image is resized to 512 x 512, where data augmentation operations include random horizontal flips, random affine transformations, random color space Jittering (saturation and intensity), and Gaussian blur. The maximum length of referring expression is set to 40, where the [CLS] and [SEP] tokens are inserted into the referring expression. For the input image and referring expression, we use two masks

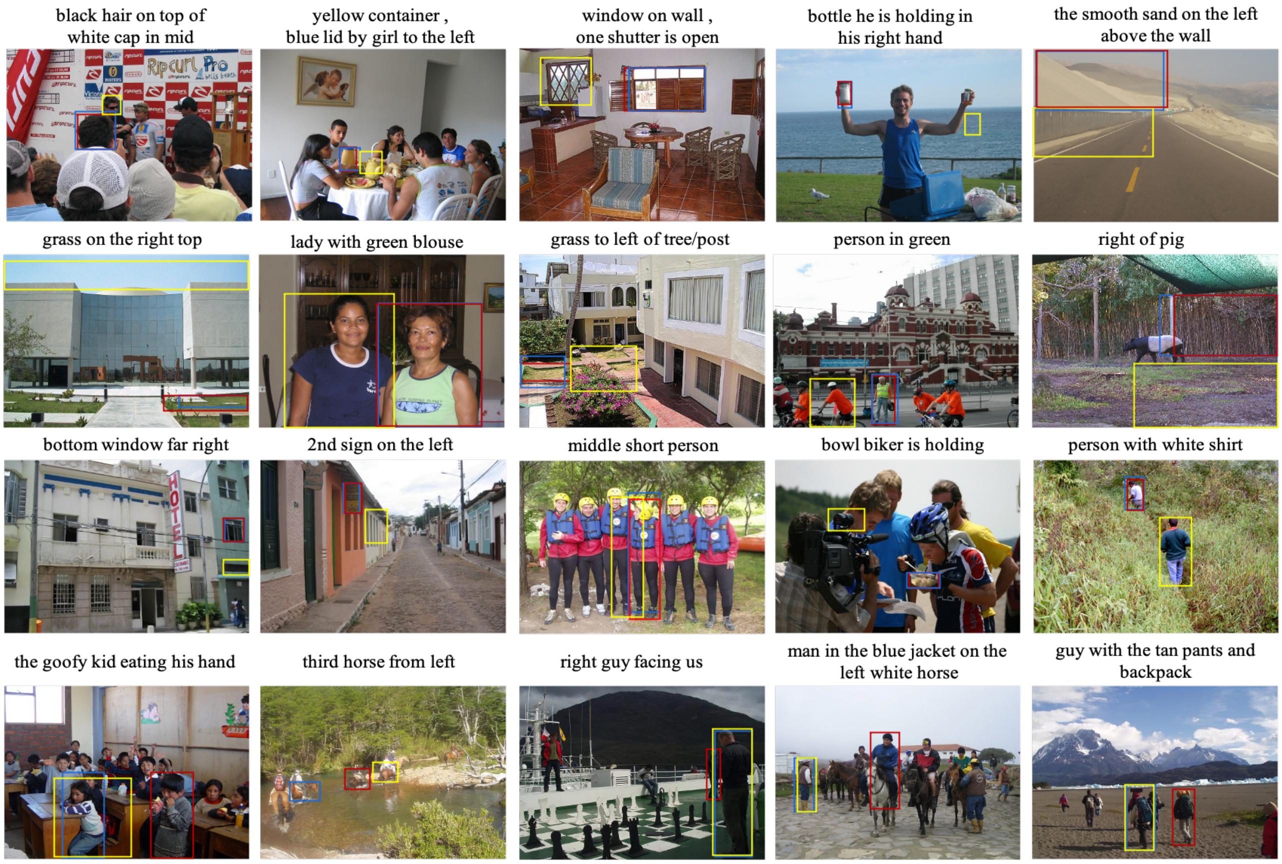

Figure 4: Qualitative results of the proposed CMF on the ReferItGame test set. The first to third rows represent the samples that our CMF predicts successfully, and the fourth row represents the samples that our CMF fails to predict. The blue boxes represent the prediction of our CMF, the yellow boxes represents the prediction of the baseline, and the red boxes are the corresponding ground-truths. Best viewed in color.

to record the padded pixels and words respectively, which do not participate in the computation of the transformers. We implement our framework with PyTorch [41] and conduct experiments with eight NVIDIA A100 GPUs.

Inference. The input image is resized to 512 x 512 and the maximum length of referring expression is set to 40. There is no data augmentation during inference. Our framework directly outputs the coordinates of the target box without any post-processing operations.

4.3 Comparisons with State-of-the-art Methods

To verify the effectiveness of our proposed framework, we report the performance on the widely-used RefCOCO [55], RefCOCO+ [55], RefCOCOg [36], and ReferItGame [23] datasets and compare with the state-of-the-art methods including one-stage methods [8, 11, 27, 42, 51, 52, 58], two-stage methods [3, 17, 31, 54, 57], and multi-task learning methods [25, 35, 47] with referring expression segmentation (RES) or referring expression generation (REG). Furthermore, we also compare the performance with state-of-the-art methods [8, 51] under different lengths of referring expression.

Table 1 shows the comparison of our framework with state-of-the-art one-stage methods [8, 11, 27, 42, 51, 52, 58]. We observe a substantial performance boost of +3.57%/ +4.21%/ +1.59% on RefCOCO, +6.84%/ +5.73%/ +6.15% on RefCOCO+, +5.52%/ +6.62%/ +5.59% on RefCOCOg, and +3.20% on ReferItGame. Our method outperforms the high-performance TransVG [8], which only uses visual and textual features of the last layer extracted from visual and language encoders. Unlike TransVG [8], our method exploits the rich hierarchical information contained in visual and language encoders and effectively achieves cross-level multi-modal fusion to improve REC performance.

A comparison of our framework with state-of-the-art two-stage methods [3, 17, 31, 54, 57] is shown in Table 1. We find that the performance improvement of RefCOCO is +3.89%/ +3.33%/ +3.90%, RefCOCO+ is +5.39%/ +4.58%/ +3.82%, RefCOCOg is +7.92%/ +5.78% / +4.05%, and ReferItGame is +10.93%. Compared with the two-stage methods, our method is not affected by the accuracy of the candidate boxes, and the correctness of the matching between the candidate boxes and the referring expressions. In particular, unlike previous one-stage and two-stage methods whose performance

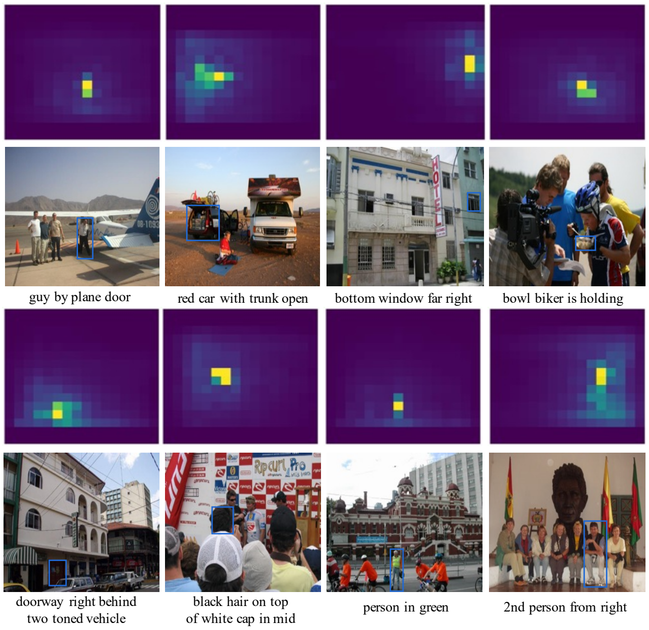

Figure 5: Visualization of the [REG] token's attention score on the ReferItGame test set. The blue boxes represent the prediction of CMF.

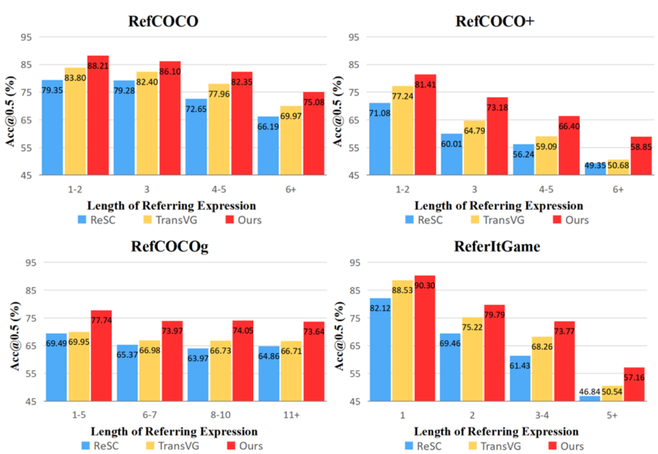

Figure 6: Comparison with state-of-the-art methods [8, 51] under different lengths of referring expression on RefCOCO [55], RefCOCO+ [55], RefCOCOg [36] and ReferItGame [23] test sets, where the test sets of RefCOCO and RefCOCO+ contain testA and testB sets.

is comparable, our one-stage method significantly outperforms two-stage methods.

Besides, Table 1 also shows the comparison of our method with state-of-the-art multi-task learning methods [25, 35, 47]. MCN [35] and RT [25] are multi-task learning methods including REC and RES while PFOS [47] is multi-task learning method including REC and REG. We observe the performance improvement of +2.36%/ +1.74%/ +3.37% on RefCOCO, +2.06%/ +2.30%/ +1.08% on RefCOCO+, +8.01%/ +6.92%/ +5.27% on RefCOCOg, and +2.51% on ReferItGame. Compared with the multi-task learning methods, our method achieves better performance.

Furthermore, Fig. 6 shows the performance comparison of state-of-the-art methods [8, 51] under different lengths of referring expression, where TransVG [8] and ReSC [51] methods that open source the models are selected for comparison. We observe a substantial performance boost of +4.41%/ +3.70%/ +4.39%/ +5.11% on RefCOCO, +4.17%/ +8.39%/ +7.31%/ +8.17% on RefCOCO+, +7.79%/ +6.99%/ +7.32%/ +6.93% on RefCOCOg and +1.77%/ +4.57%/ +5.51%/ +6.62% on ReferItGame from short to long referring expressions.

4.4 Ablation Analysis

In this section, we conduct a series of ablation studies to further investigate the relative importance and specific contributions of each component in our proposed framework. We use ResNet50 [16] and the uncased base of 12-layer BERT [9] as the visual and language encoders, respectively, to conduct ablation experiments on the val set of ReferItGame.

Effectiveness of each main component in our framework. We study the effectiveness of each main module in our framework, as illustrated in Table 2. "$\{F_v^i\}_{i=1}^4$" means using multi-layer visual features extracted from ResNet50. "LAFM" means using language-adaptive fusion module. "VLIM(One Layer)" means using the visual-language interaction module including a stack of one transformer encoder layer. "VLIM(Two Layers)" means using the visual-language interaction module including a stack of two transformer encoder layers. To be specific, our baseline inputs features of the last layer extracted from visual and language encoders into the visual-language fusion module (VLFM), and uses [REG] token output by the VLFM to directly predict the target box through a three-layer perceptron.

The result in the first row of the Table 2 is used as the baseline. From the second row of the Table 2, we find that replacing visual features of the last layer with multi-layer visual features can improve the performance. Based on the experiment in the second row of the Table 2, we equip visual features of each layer with "VLIM (One Layer)", where the textual features are extracted from the last layer of BERT. We observe that grouping multi-modal interaction can effectively improve performance. According to the fourth rows of the Table 2, language-adaptive fusion module can assign adaptively fused textual features to the corresponding visual features for multi-modal interaction and further improve accuracy. In addition, we can observe that using the visual-language interaction module of more layers makes the network performance slightly improved, as shown in the fifth row of the Table 2.

Design of the language-adaptive fusion module. We study the design of the language-adaptive fusion module (LAFM), and report the results in Table 3. For the sake of fairness, all comparison methods use multi-layer visual features $\{F_v^i\}_{i=1}^4$ and visual-language interaction module including a stack of one transformer encoder layer. There are several designs to construct the LAFM. We detail these designs and analysis them as follows:

- *Textual Features of Last Layer.* We only use textual features of the last layer extracted from N-layer language encoder.

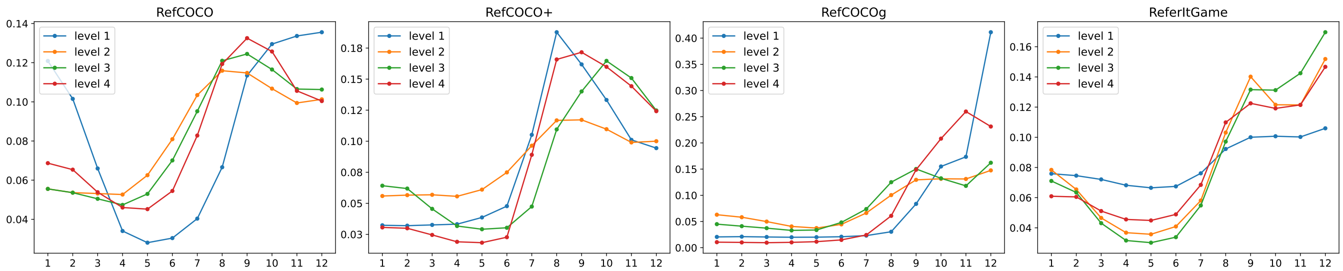

Figure 7: Visualizations of the LAFM adaptive fusion weights. The test sets of RefCOCO [55], RefCOCO+ [55], RefCOCOg [36] and ReferItGame [23] are used for visualization. The horizontal axis represents textual features extracted from low layers to high layers. Blue, orange, green and red lines represent visual features extracted from shallow layers to deep layers.

– *N Learnable Parameters + Softmax.* We set N learnable parameters and optimize them end-to-end with the framework. After softmax normalization, we perform a weighted sum of N-layer textual features to obtain the fused textual features.
– *CLS + Softmax.* We obtain $q \in \mathbb{R}^{N \times Q}$ using the [CLS] token of the N-layer textual features. Then, we use the Eq. (3) and softmax operation to get the normalized N-dimensional vector, which is used to calculate the weighted sum of textual features.
– *CLS + Self-Attention + Softmax.* Based on the third design, we add language-level self-attention to establish the affinity matrix $a \in \mathbb{R}^{N \times N}$. After this designed module, we can obtain the adaptively fused textual features.
– *MAX + Self-Attention + Softmax.* Different from the fourth design, we perform max pooling over N-layer textual features to obtain $q \in \mathbb{R}^{N \times Q}$.
– *MEAN + Self-Attention + Softmax.* Different from the fourth design, we perform average pooling over N-layer textual features to obtain $q \in \mathbb{R}^{N \times Q}$.

To be specific, we take the first row of result in Table 3 as the baseline. From the second row of the Table 3, we can find that directly optimizing N learnable parameters and obtaining textual features by weighted fusion cannot significantly improve the performance. We gradually design the architectures, as shown in the third and fourth rows of Table 3. From the experimental result in the fourth row of Table 3, our designed architecture can establish the association between textual features of different layers and effectively utilize the hierarchical information contained in the language encoder to improve REC performance. In addition, we also supplement the experiments using average pooling, and max pooling operations to obtain $q \in \mathbb{R}^{N \times Q}$, as shown in the fifth and sixth rows of the Table 3. We find that compared with average pooling and max pooling operations, using [CLS] token can significantly improve network performance.

4.5 Qualitative Results

To better demonstrate the effectiveness of our proposed method, we show the visualization results of our CMF and the baseline on the ReferItGame test set, as shown in Fig. 4. Specifically, our proposed CMF utilizes visual and textual features of different layers contained in visual and language encoders while the baseline only uses features extracted from the last layer of visual and language encoders. The first to third rows of the Fig. 4 represent examples where our CMF predicts successfully but the baseline fails. From the first row to the third row of the Fig. 4, we can observe that our CMF can effectively utilize visual and textual hierarchical information to accurately locate target objects. Despite the good results, there are some failures in our model, as shown in fourth row of the Fig. 4. This shows that our model still faces challenges when faced with complex visual scenes or referring expressions. We also visualize the attention score of the [REG] token, as shown in Fig. 5. [REG] token incorporates the hierarchical information of visual and textual features, and accurately locates the visual region corresponding to the referring expression.

Furthermore, we supplement the visualization of LAFM adaptive fusion weights, as shown in Fig. 7. The test sets of RefCOCO [55], RefCOCO+ [55], RefCOCOg [36] and ReferItGame [23] are used for visualization, where the test sets of RefCOCO and RefCOCO+ contain testA and testB sets. As shown in Fig. 7, we can observe that visual features at different layers in each dataset have various adaptive fusion weights for textual features. Compared to most state-of-the-art methods [8, 11, 22, 25, 47, 51] that only use textual features from the last layer of the language encoder, our method utilizes LAFM to adaptively generate textual features for visual features of each layer.

5 CONCLUSIONS

In this paper, we propose to effectively utilize the inherent hierarchical information contained in visual and language encoders for accurate language-to-visual localization. We design a Cross-level Multimodal Fusion framework named CMF to gradually integrates rich hierarchical visual and textual information. In this framework, we first design a language-adaptive fusion module (LAFM) to construct adaptively fused textual features for visual features of each layer. Then, we propose two successive processes, *i.e.* grouping multimodal interaction and cross-level multi-modal fusion, to achieve better intra- and inter-modal fusion. The framework effectively utilizes the rich hierarchical information contained in visual and language encoders, and achieves REC with better performance. Extensive experiments have demonstrated the effectiveness of our framework. In the future, we will continue to explore the effective utilization of the rich hierarchical information contained in visual and language encoders.

REFERENCES

[1] Stanislaw Antol, Aishwarya Agrawal, Jiasen Lu, Margaret Mitchell, Dhruv Batra, C Lawrence Zitnick, and Devi Parikh. 2015. Vqa: Visual question answering. In *ICCV*. 2425–2433.

[2] Nicolas Carion, Francisco Massa, Gabriel Synnaeve, Nicolas Usunier, Alexander Kirillov, and Sergey Zagoruyko. 2020. End-to-end object detection with transformers. In *ECCV*. 213–229.

[3] Long Chen, Wenbo Ma, Jun Xiao, Hanwang Zhang, and Shih-Fu Chang. 2021. Ref-NMS: breaking proposal bottlenecks in two-stage referring expression grounding. In *AAAI*. 1036–1044.

[4] Yen-Chun Chen, Linjie Li, Licheng Yu, Ahmed El Kholy, Faisal Ahmed, Zhe Gan, Yu Cheng, and Jingjing Liu. 2020. Uniter: Universal image-text representation learning. In *ECCV*. 104–120.

[5] Bowen Cheng, Alex Schwing, and Alexander Kirillov. 2021. Per-pixel classification is not all you need for semantic segmentation. In *NeurIPS*.

[6] Zihang Dai, Zhilin Yang, Yiming Yang, Jaime Carbonell, Quoc V Le, and Ruslan Salakhutdinov. 2019. Transformer-xl: Attentive language models beyond a fixed-length context. *arXiv preprint arXiv:1901.02860* (2019).

[7] Mostafa Dehghani, Stephan Gouws, Oriol Vinyals, Jakob Uszkoreit, and Łukasz Kaiser. 2018. Universal transformers. *arXiv preprint arXiv:1807.03819* (2018).

[8] Jiajun Deng, Zhengyuan Yang, Tianlang Chen, Wengang Zhou, and Houqiang Li. 2021. Transvg: End-to-end visual grounding with transformers. In *ICCV*. 1769–1779.

[9] Jacob Devlin, Ming-Wei Chang, Kenton Lee, and Kristina Toutanova. 2018. Bert: Pre-training of deep bidirectional transformers for language understanding. *arXiv preprint arXiv:1810.04805* (2018).

[10] Alexey Dosovitskiy, Lucas Beyer, Alexander Kolesnikov, Dirk Weissenborn, Xiaohua Zhai, Thomas Unterthiner, Mostafa Dehghani, Matthias Minderer, Georg Heigold, Sylvain Gelly, et al. 2020. An image is worth 16x16 words: Transformers for image recognition at scale. *arXiv preprint arXiv:2010.11929* (2020).

[11] Ye Du, Zehua Fu, Qingjie Liu, and Yunhong Wang. 2021. Visual grounding with transformers. *arXiv preprint arXiv:2105.04281* (2021).

[12] Hugo Jair Escalante, Carlos A Hernández, Jesus A Gonzalez, Aurelio López-López, Manuel Montes, Eduardo F Morales, L Enrique Sucar, Luis Villasenor, and Michael Grubinger. 2010. The segmented and annotated IAPR TC-12 benchmark. *Computer vision and image understanding* 114, 4 (2010), 419–428.

[13] Chuang Gan, Yandong Li, Haoxiang Li, Chen Sun, and Boqing Gong. 2017. Vqs: Linking segmentations to questions and answers for supervised attention in vqa and question-focused semantic segmentation. In *ICCV*. 1811–1820.

[14] Bharath Hariharan, Pablo Arbeláez, Ross Girshick, and Jitendra Malik. 2015. Hypercolumns for object segmentation and fine-grained localization. In *CVPR*. 447–456.

[15] Kaiming He, Georgia Gkioxari, Piotr Dollár, and Ross Girshick. 2017. Mask r-cnn. In *ICCV*. 2961–2969.

[16] Kaiming He, Xiangyu Zhang, Shaoqing Ren, and Jian Sun. 2016. Deep residual learning for image recognition. In *CVPR*. 770–778.

[17] Richang Hong, Daqing Liu, Xiaoyu Mo, Xiangnan He, and Hanwang Zhang. 2019. Learning to compose and reason with language tree structures for visual grounding. *IEEE transactions on pattern analysis and machine intelligence* (2019).

[18] Ronghang Hu, Marcus Rohrbach, Jacob Andreas, Trevor Darrell, and Kate Saenko. 2017. Modeling relationships in referential expressions with compositional modular networks. In *CVPR*. 1115–1124.

[19] Ronghang Hu, Huazhe Xu, Marcus Rohrbach, Jiashi Feng, Kate Saenko, and Trevor Darrell. 2016. Natural language object retrieval. In *CVPR*. 4555–4564.

[20] Sergey Ioffe and Christian Szegedy. 2015. Batch normalization: Accelerating deep network training by reducing internal covariate shift. In *ICML*. 448–456.

[21] Ganesh Jawahar, Benoît Sagot, and Djamé Seddah. 2019. What does BERT learn about the structure of language?. In *ACL*.

[22] Aishwarya Kamath, Mannat Singh, Yann LeCun, Gabriel Synnaeve, Ishan Misra, and Nicolas Carion. 2021. MDETR-modulated detection for end-to-end multi-modal understanding. In *ICCV*. 1780–1790.

[23] Sahar Kazemzadeh, Vicente Ordonez, Mark Matten, and Tamara Berg. 2014. Referitgame: Referring to objects in photographs of natural scenes. In *EMNLP*. 787–798.

[24] Alex Krizhevsky, Ilya Sutskever, and Geoffrey E Hinton. 2012. Imagenet classification with deep convolutional neural networks. In *NeurIPS*.

[25] Muchen Li and Leonid Sigal. 2021. Referring transformer: A one-step approach to multi-task visual grounding. In *NeurIPS*.

[26] Xiujun Li, Xi Yin, Chunyuan Li, Pengchuan Zhang, Xiaowei Hu, Lei Zhang, Lijuan Wang, Houdong Hu, Li Dong, Furu Wei, et al. 2020. Oscar: Object-semantics aligned pre-training for vision-language tasks. In *ECCV*. 121–137.

[27] Yue Liao, Si Liu, Guanbin Li, Fei Wang, Yanjie Chen, Chen Qian, and Bo Li. 2020. A real-time cross-modality correlation filtering method for referring expression comprehension. In *CVPR*. 10880–10889.

[28] Tsung-Yi Lin, Michael Maire, Serge Belongie, James Hays, Pietro Perona, Deva Ramanan, Piotr Dollár, and C Lawrence Zitnick. 2014. Microsoft coco: Common objects in context. In *ECCV*. 740–755.

[29] Daqing Liu, Hanwang Zhang, Feng Wu, and Zheng-Jun Zha. 2019. Learning to assemble neural module tree networks for visual grounding. In *ICCV*. 4673–4682.

[30] Wei Liu, Dragomir Anguelov, Dumitru Erhan, Christian Szegedy, Scott Reed, Cheng-Yang Fu, and Alexander C Berg. 2016. Ssd: Single shot multibox detector. In *ECCV*. 21–37.

[31] Xihui Liu, Zihao Wang, Jing Shao, Xiaogang Wang, and Hongsheng Li. 2019. Improving referring expression grounding with cross-modal attention-guided erasing. In *CVPR*. 1950–1959.

[32] Ze Liu, Yutong Lin, Yue Cao, Han Hu, Yixuan Wei, Zheng Zhang, Stephen Lin, and Baining Guo. 2021. Swin transformer: Hierarchical vision transformer using shifted windows. In *ICCV*. 10012–10022.

[33] Ilya Loshchilov and Frank Hutter. 2017. Decoupled weight decay regularization. *arXiv preprint arXiv:1711.05101* (2017).

[34] Jiasen Lu, Dhruv Batra, Devi Parikh, and Stefan Lee. 2019. Vilbert: Pretraining task-agnostic visiolinguistic representations for vision-and-language tasks. In *NeurIPS*.

[35] Gen Luo, Yiyi Zhou, Xiaoshuai Sun, Liujuan Cao, Chenglin Wu, Cheng Deng, and Rongrong Ji. 2020. Multi-task collaborative network for joint referring expression comprehension and segmentation. In *CVPR*. 10034–10043.

[36] Junhua Mao, Jonathan Huang, Alexander Toshev, Oana Camburu, Alan L Yuille, and Kevin Murphy. 2016. Generation and comprehension of unambiguous object descriptions. In *CVPR*. 11–20.

[37] Junhua Mao, Jonathan Huang, Alexander Toshev, Oana Camburu, Alan L Yuille, and Kevin Murphy. 2016. Generation and comprehension of unambiguous object descriptions. In *CVPR*. 11–20.

[38] Varun K Nagaraja, Vlad I Morariu, and Larry S Davis. 2016. Modeling context between objects for referring expression understanding. In *ECCV*. 792–807.

[39] Yingwei Pan, Ting Yao, Yehao Li, and Tao Mei. 2020. X-linear attention networks for image captioning. In *CVPR*. 10971–10980.

[40] Niki Parmar, Ashish Vaswani, Jakob Uszkoreit, Lukasz Kaiser, Noam Shazeer, Alexander Ku, and Dustin Tran. 2018. Image transformer. In *ICML*. 4055–4064.

[41] Adam Paszke, Sam Gross, Soumith Chintala, Gregory Chanan, Edward Yang, Zachary DeVito, Zeming Lin, Alban Desmaison, Luca Antiga, and Adam Lerer. 2017. Automatic differentiation in pytorch. (2017).

[42] Heqian Qiu, Hongliang Li, Qingbo Wu, Fanman Meng, Hengcan Shi, Taijin Zhao, and King Ngi Ngan. 2020. Language-aware fine-grained object representation for referring expression comprehension. In *ACM MM*. 4171–4180.

[43] Shaoqing Ren, Kaiming He, Ross Girshick, and Jian Sun. 2015. Faster r-cnn: Towards real-time object detection with region proposal networks. In *NeurIPS*.

[44] Hamid Rezatofighi, Nathan Tsoi, JunYoung Gwak, Amir Sadeghian, Ian Reid, and Silvio Savarese. 2019. Generalized intersection over union: A metric and a loss for bounding box regression. In *CVPR*. 658–666.

[45] Anna Rohrbach, Marcus Rohrbach, Ronghang Hu, Trevor Darrell, and Bernt Schiele. 2016. Grounding of textual phrases in images by reconstruction. In *ECCV*. 817–834.

[46] Amaia Salvador, Xavier Giró-i Nieto, Ferran Marqués, and Shin'ichi Satoh. 2016. Faster r-cnn features for instance search. In *CVPR*. 9–16.

[47] Mengyang Sun, Wei Suo, Peng Wang, Yanning Zhang, and Qi Wu. 2022. A proposal-free one-stage framework for referring expression comprehension and generation via dense cross-attention. *IEEE Transactions on Multimedia* (2022).

[48] Ashish Vaswani, Noam Shazeer, Niki Parmar, Jakob Uszkoreit, Llion Jones, Aidan N Gomez, Łukasz Kaiser, and Illia Polosukhin. 2017. Attention is all you need. In *NeurIPS*.

[49] Huiyu Wang, Yukun Zhu, Hartwig Adam, Alan Yuille, and Liang-Chieh Chen. 2021. Max-deeplab: End-to-end panoptic segmentation with mask transformers. In *CVPR*. 5463–5474.

[50] Peng Wang, Dongyang Liu, Hui Li, and Qi Wu. 2020. Give me something to eat: referring expression comprehension with commonsense knowledge. In *ACM MM*. 28–36.

[51] Zhengyuan Yang, Tianlang Chen, Liwei Wang, and Jiebo Luo. 2020. Improving one-stage visual grounding by recursive sub-query construction. In *ECCV*. 387–404.

[52] Zhengyuan Yang, Boqing Gong, Liwei Wang, Wenbing Huang, Dong Yu, and Jiebo Luo. 2019. A fast and accurate one-stage approach to visual grounding. In *ICCV*. 4683–4693.

[53] Quanzeng You, Hailin Jin, Zhaowen Wang, Chen Fang, and Jiebo Luo. 2016. Image captioning with semantic attention. In *CVPR*. 4651–4659.

[54] Licheng Yu, Zhe Lin, Xiaohui Shen, Jimei Yang, Xin Lu, Mohit Bansal, and Tamara L Berg. 2018. Mattnet: Modular attention network for referring expression comprehension. In *CVPR*. 1307–1315.

[55] Licheng Yu, Patrick Poirson, Shan Yang, Alexander C Berg, and Tamara L Berg. 2016. Modeling context in referring expressions. In *ECCV*. 69–85.

[56] Wei Yu, Kuiyuan Yang, Hongxun Yao, Xiaoshuai Sun, and Pengfei Xu. 2017. Exploiting the complementary strengths of multi-layer CNN features for image retrieval. *Neurocomputing* 237 (2017), 235–241.

[57] Zhou Yu, Jun Yu, Chenchao Xiang, Zhou Zhao, Qi Tian, and Dacheng Tao. 2018. Rethinking diversified and discriminative proposal generation for visual grounding. *arXiv preprint arXiv:1805.03508* (2018).

[58] Yiyi Zhou, Rongrong Ji, Gen Luo, Xiaoshuai Sun, Jinsong Su, Xinghao Ding, Chia-Wen Lin, and Qi Tian. 2021. A real-time global inference network for one-stage referring expression comprehension. *IEEE Transactions on Neural Networks and Learning Systems* (2021).

[59] Jinhua Zhu, Yingce Xia, Lijun Wu, Di He, Tao Qin, Wengang Zhou, Houqiang Li, and Tie-Yan Liu. 2020. Incorporating bert into neural machine translation. *arXiv preprint arXiv:2002.06823* (2020).

[60] Xizhou Zhu, Weijie Su, Lewei Lu, Bin Li, Xiaogang Wang, and Jifeng Dai. 2020. Deformable detr: Deformable transformers for end-to-end object detection. *arXiv preprint arXiv:2010.04159* (2020).

[61] Yuke Zhu, Oliver Groth, Michael Bernstein, and Li Fei-Fei. 2016. Visual7w: Grounded question answering in images. In *CVPR*. 4995–5004.